Magn Reson Med Sci 2019; 18; 134–141
doi:10.2463/mrms.mp.2018-0003
Published Online: July 26, 2018

MAJOR PAPER

Assessment of Coronary Flow Velocity Reserve in the Left Main Trunk Using Phase-contrast MR Imaging at 3T: Comparison with ^{15}O-labeled Water Positron Emission Tomography

Yasuka Kikuchi[1,2], Masanao Naya[3*], Noriko Oyama-Manabe[2], Osamu Manabe[4], Hiroyuki Sugimori[5], Kohsuke Kudo[2], Fumi Kato[2], Tadao Aikawa[3], Hiroyuki Tsutsui[6], Nagara Tamaki[7], and Hiroki Shirato[8]

Purpose: The aim of this study was to verify coronary flow velocity reserve (CFVR) on the left main trunk (LMT) in comparison with myocardial flow reserve (MFR) by ^{15}O-labeled water positron emission tomography (PET) (MFR-PET) in both the healthy adults and the patients with coronary artery disease (CAD), and to evaluate the feasibility of CFVR to detect CAD.

Methods: Eighteen healthy adults and 13 patients with CAD were evaluated. CFVR in LMT was estimated by 3T magnetic resonance imaging (MRI) with phase contrast technique. MFR-PET in the LMT territory including anterior descending artery and circumflex artery was calculated as the ratio of myocardial blood flow (MBF)-PET at stress to MBF-PET at rest.

Results: There was a significant positive relationship between CFVR and MFR-PET ($R = 0.45$, $P < 0.0001$). Inter-observer calculations of CFVR showed good correlation ($R^2 = 0.93$, $P < 0.0001$). The CFVR in patients with CAD was significantly lower than that in healthy adults (1.90 ± 0.61 vs. 2.77 ± 1.03, respectively, $P = 0.01$), which were similar to the results of MFR-PET (2.23 ± 0.84 vs. 3.96 ± 1.04, respectively, $P < 0.0001$). For the detection of patients with CAD, the area under the curve was 0.78 ($P = 0.01$). The sensitivity was 0.77 and specificity was 0.72 when a cut-off of 2.15 was used.

Conclusion: CFVR by 3T was validated with MFR-PET. CFVR could detect the patients with CAD. This method is a simple and reliable index without radiation or contrast material.

Keywords: *coronary artery disease, coronary flow velocity reserve, magnetic resonance imaging, phase contrast, 3 tesla*

Introduction

There is growing evidence that stress perfusion imaging can detect functional myocardial ischemia in patients with coronary artery disease (CAD).[1–3] Recent studies have demonstrated that quantitative myocardial flow reserve (MFR), which is calculated by dividing myocardial blood flow (MBF, ml/g/min) at stress by MBF at rest on positron emission tomography (PET), is reliable for detection of CAD and for excluding significant multi-vessel CAD with very high relative predictive values.[4]

Coronary flow velocity reserve (CFVR) estimated from velocity of coronary arteries during stress and at rest by using Doppler echocardiography or intracoronary Doppler guidewire has been used to assess CAD.[5–8] In that regard, Sakuma et al.[9] reported an estimation of CFVR in the left anterior descending coronary artery (LAD) using 1.5T magnetic resonance imaging (MRI) with phase contrast (PC) technique; importantly, this technique does not require the injection of contrast material. In healthy volunteers, CFVR is also correlated with MFR values obtained by ^{15}O-labeled water PET which is a gold standard for quantifying MBF. However, CFVR has not yet been validated in 3T MRI or in patients with CAD. In addition, they assessed only LAD lesion in the

[1]Center for Cause of Death Investigation, Faculty of Medicine, Hokkaido University, Hokkaido, Japan
[2]Department of Diagnostic and Interventional Radiology, Hokkaido University Hospital, Hokkaido, Japan
[3]Department of Cardiovascular Medicine, Hokkaido University Graduate School of Medicine, N15 W7 Kita-ku, Sapporo, Hokkaido 060-8638, Japan
[4]Department of Nuclear Medicine, Hokkaido University Graduate School of Medicine, Hokkaido, Japan
[5]Faculty of Health Sciences, Hokkaido University, Hokkaido, Japan
[6]Department of Cardiovascular Medicine, Kyushu University, Fukuoka, Japan
[7]Department of Radiology, Kyoto Prefectural University of Medicine, Kyoto, Japan
[8]Department of Radiation Medicine, Hokkaido University Graduate School of Medicine, Hokkaido, Japan

*Corresponding author, Phone: +81-11-706-6974, Fax: +81-11-706-7874, E-mail: naya@med.hokudai.ac.jp

Received: January 9, 2018 | Accepted: May 23, 2018

previous study. Because the left main trunk (LMT) lesion supplies major part of the left ventricle,[10] it is important to evaluate CFVR on the LMT. In fact, Han et al.[11] reported that CFVR in the LMT was decreased, even if it was measured at the proximal site to the coronary stenosis.

The aim of this study was to establish the CFVR on LMT lesion using PC technique on 3T MRI in comparison with the MFR by ^{15}O-labeled water PET (MFR-PET) in both healthy adults and patients with CAD.

Materials and Methods

Subjects

The Institutional Review Board approved this study. Written informed consent for MRI and PET studies were obtained from all subjects, but informed consent for this study was waived due to its retrospective nature.

Twenty healthy adults with no history of CAD from June to December 2010 and 16 patients with invasive coronary angiography (ICA) confirmed CAD (>50% coronary artery stenosis assessed visually) from July to November 2015 were enrolled in this study. All of them underwent PC MRI and ^{15}O-labeled water PET in random order under both stress and rest status within 4 weeks at Hokkaido University Hospital. Data for healthy adults were retrieved from the previous study.[12] Initial two healthy adults were excluded due to use the different velocity window from the rest. Three patients with CAD were excluded because it was difficult to identify the short axis view of LMT using magnitude images in some phases through the cardiac cycle. Ultimately, 18 healthy adults (age; 28.6 ± 8.9 year, all male) and 13 patients with CAD (age; 67.2 ± 12.7 year, 8 male) were analyzed. The LMT territory includes LMT (#5), LAD (#6-10), and left circumflex artery (LCx) (#11-15). Among 13 patients with CAD, 8 patients had 1-vessel disease (VD) (5 with LAD, 3 with LCx) and 5 patients with CAD had 2-VD (in both LAD and LCx). No patients had LMT disease (Table 1). All subjects refrained from caffeine-containing beverage consumption for at least 24 h, and from smoking for at least 4 h prior to the MRI and PET studies.

Table 1 Baseline characteristics

	Healthy adults (n = 18)	Patients with CAD (n = 13)
Age (years)	28.6 ± 8.9	67.2 ± 12.7
Gender (male/female)	18/0	8/5
BMI (kg/m^2)	22.3 ± 3.5	23.6 ± 3.8
Smoking (%)	7 (39)	10 (77)
Hypertension (%)	0 (0)	10 (77)
Hyperlipidemia (%)	1 (5)	10 (77)
Diabetes mellitus (%)	0 (0)	9 (69)
History of myocardial infarction (%)	0 (0)	5 (38)
CAD severity (%)		
0-VD	-	0 (0)
1-VD (LAD or LCx)	-	8 (62)
2-VD (LAD and LCx)	-	5 (38)
LMT	-	0 (0)

CAD, coronary artery disease; BMI, body mass index; VD, vessel disease; LAD, left anterior descending coronary artery; LCx, left circumflex artery; LMT, left main trunk; -, not available.

MR protocol

Magnetic resonance acquisition was performed using a 3T whole-body scanner (Achieva Tx; Philips Medical Systems, Best, The Netherlands) with a 32-channel phased-array receiver torso-cardiac coil. A fully flexible dual-source radiofrequency transmission system for patient-adaptive local radiofrequency shimming was used. This achieves optimal B_1 homogeneity, even with a moving heart.[13] In addition to cine image, PC scans were obtained during adenosine triphosphate (ATP) stress status and at rest. ATP at 160 μg/kg/min was started 3 min before acquiring stress images. Electrocardiogram (ECG) leads were attached to the chest for cardiac gating and were monitored. Blood pressure was also monitored during the examinations. Heart rate (HR), systolic blood pressure (sBP), and diastolic blood pressure (dBP) were measured three times at pre-ATP injection, 3 min after ATP injection, and before the rest scan. The rate pressure product (RPP) was calculated to multiply sBP and HR.

Measurement of CFVR using PC MRI

Breath-holding cine images were acquired on coronal, axial, and oblique planes as scout images for the localization of the LMT. These scout images were acquired with a section thickness of 8 mm, a TR of 3.5 ms, a TE of 1.7 ms, a FOV of 380 × 380 mm^2, frequency-encoding resolution of 256, phase-encoding step numbers of 256, a reconstructed image matrix of 256 × 256, and a pixel dimension of approximately 1.48 × 1.48 mm^2.

A velocity-encoded fast gradient echo sequence with *k*-space segmentation was used for flow measurement. Oblique PC MRI were acquired on an imaging plane perpendicular to the LMT (Fig. 1), with a section thickness of 6 mm, TR of 3.9 ms, TE of 2.7 ms, FOV of 400 × 400 mm^2, base frequency-encoding resolution of 215, base phase-encoding step numbers of 215, interpolated reconstructed image matrix of 320 × 320 from base resolution, and pixel dimension of approximately 1.25 × 1.25 mm^2. The net spatial resolution of PC MRI was 400 mm/215 pixels. Sensitivity Encoding (SENSE) factor is 2. Uniform radiofrequency excitation was used in this sequence, which maintains the spins in steady state, eliminates the need for dummy excitations before data collection, and enables the acquisition of data immediately after the ECG R wave trigger. Velocity-encoding gradients were applied in a slice-selective direction. A velocity window

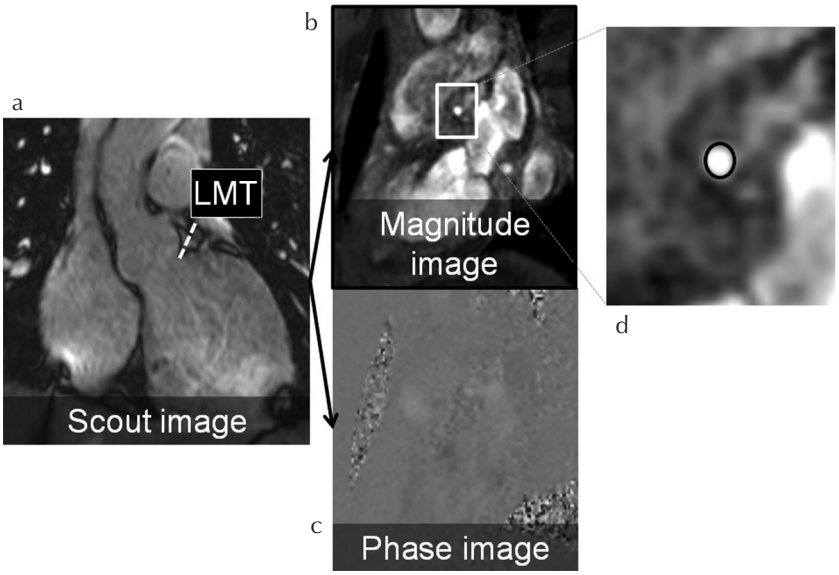

Fig. 1 The methods of setting the ROIs in left main trunk (LMT). (**a**) A scout image, namely an oblique image acquired on the imaging plane perpendicular to the LMT. (**b**) A magnitude image obtained from the scout image and used to set the ROIs in this study. (**c**) A phase-difference cine image, also obtained from the scout image. (**d**) ROIs for each of 23 phases on the short axis were set semi-automatically using the magnitude image.

of ±150 cm/s at stress and 70 cm/s at rest was used for flow velocity measurement in the LMT, which was modified from those reported in the previous studies.[14] Four lines in *k*-space were collected per trigger per segment. For each *k*-space image, positive and negative velocity-encoding data were acquired as a sequential pair. The true temporal resolution, the time during which imaging data were acquired for each cine frame, was 17-20 s. The magnitude and phase-difference cine images with 23 temporal phases were reconstructed from the data acquired in a single breath hold. After the subjects took a deep breath in and breathed out, PC MRI data were acquired with suspended shallow inspiration for 17-20 s.

For flow analysis, the MRI data were transferred from the MR scanner to an extended workstation (Early Warning Scoring; Philips, Best, The Netherlands). Using magnitude images, we placed small ROIs with the dimension of the vessel diameter on individual cine frames to correct in-plane movement that might occur during the cardiac cycle. The measurements were repeated for all cardiac phases, using a magnitude image as a reference. Peak-velocity was calculated from the velocity curve at stress and rest, respectively, and CFVR was calculated by dividing peak-velocity during stress by that at rest.

^{15}O-labeled water PET scan

After obtaining a transmission scan, rest and stress examinations (same ATP dose as for MRI) were performed. We used two types of PET scan due to the replacement of PET scanners during the study period.

Healthy adults

Dynamic ^{15}O-labeled water PET data were acquired using HR + PET scanner (Siemens, Erlangen, Germany). All emissions and transmissions were acquired in the two-dimensional mode. A 5-min transmission scan was acquired for the attenuation correction of all subsequent emission scans. ^{15}O-water (1500 MBq) was gradually infused (over 100 s) into the antecubital vein and the 20 frames dynamic PET scan comprising 6 × 5 s, 6 × 15 s, and 8 × 30 s frames were acquired over 6-min. PET images were reconstructed using a filtered back-projection algorithm with a Hanning filter (cut-off; 0.4) (ECAT v7.2; Siemens). The frames included 63 trans-axial slices (matrix size; 128 × 128, voxel size; 3.4 × 3.4 × 2.4 mm).

Patients with CAD

Dynamic ^{15}O-labeled water PET data were acquired using a whole-body PET/CT scanner (Gemini TF PET/CT; Philips Healthcare, Cleveland, OH, USA). After a CT scanning for attenuation correction, ^{15}O-water (500 MBq) was intravenously administered simultaneously with a 6-min dynamic PET acquisition. PET images were reconstructed using the 3D row action maximum likelihood algorithm into 24-serial frames (18 × 10 s, 6 × 30 s). The frames included 45 trans-axial slices (matrix size; 144 × 144, voxel size; 4.0 × 4.0 × 4.0 mm^3).

^{15}O-labeled water PET image analysis

We calculated MBF from ROIs plotted in the left ventricular chamber and myocardium using in-house software and a previously described single-tissue compartment model.[15] MFR-PET in the LMT territory, which was based on a 16-segment model using a short axis and was determined by 11 segments excluded five right coronary artery (RCA) segments, was calculated as the average value of 11 segments as the ratio of MBF-PET during ATP-induced stress to MBF-PET at rest.

Statistical analysis

Pearson's correlation coefficients, linear regression analyses and Bland-Altman plots were used to assess the relationship

Table 2 Hemodynamics

	Healthy adults (n = 18)			Patients with CAD (n = 13)		
	MRI	^{15}O-labeled water PET	P-value	MRI	^{15}O-labeled water PET	P-value
Rest status						
sBP (mmHg)	120 ± 9	120 ± 9	0.89	137 ± 30	152 ± 17	0.17
dBP (mmHg)	71 ± 6	72 ± 6	0.84	78 ± 16	85 ± 10	0.24
HR (/min)	62 ±7	61 ± 7	0.83	63 ± 9	66 ± 9	0.36
RPP (mmHg/min)	7,939 ± 1,755	7,378 ± 1,162	0.94	8,668 ± 2,185	10,150 ± 2,171	0.10
Stress status						
sBP (mmHg)	125 ± 21	117 ± 7	0.95	136 ± 28	139 ± 19	0.71
dBP (mmHg)	71 ± 11	68 ± 6	0.93	76 ± 16	79 ± 15	0.52
HR (/min)	77 ± 12*	83 ± 11*	0.94	75 ± 9*	83 ± 15*	0.11
RPP (mmHg/min)	9,284 ± 2,555	9,698 ± 1,459	0.97	10,717 ± 2,505	11,996 ± 3,376	0.32

*P < 0.05 compared with rest HR. CAD, coronary artery disease; PET, positron-emission tomography; sBP, systolic blood pressure; dBP, diastolic blood pressure; HR, heart rate; RPP, rate pressure product.

between CFVR and MFR-PET. The inter-observer consistency of CFVR calculations was also evaluated (Y.K. and O.M., with 8 and 11 years of experience in cardiac imaging, respectively). Each of us set the ROIs and calculated the CFVR. The ROIs were traced undersized boundary including all pixels that contain only vessel and at least four pixels in diameter.[16,17] Each CFVR were compared in the inter-observer consistency. In addition, CFVR and MFR-PET in both healthy adults and patients with CAD were compared using unpaired t-test. Moreover, receiver operating characteristic (ROC) analysis of CFVR for the detection of patients with CAD was conducted. The cut-off value was determined by the maximum value of sensitivity - (1 - specificity). JMP Pro 13 (SAS Institute, Inc., Cary, NC, USA) and Prism 7 (GraphPad Software, San Diego, CA, USA) were used for data analysis. P-values less than 0.05 were considered statistically significant.

Results

Subject hemodynamics

Hemodynamics data are shown in Table 2. There were no significant differences in the HR, sBP, dBP, and RPP between MRI and ^{15}O-labeled water PET examinations. HR significantly increased from rest to the ATP-induced stress status in both MRI and ^{15}O-labeled water PET examinations.

Validation of CFVR against MFR-PET and inter-observer consistency of calculating CFVR

Pearson's correlation coefficients and linear regression analyses showed positive and significant relationship between CFVR and MFR-PET (Fig. 2). On the Bland-Altman plots, CFVR tended to be lower than MFR-PET, and all differences of MFR-PET and CFVR were within the mean ± 2 standard deviation except for one healthy adult (Fig. 3).

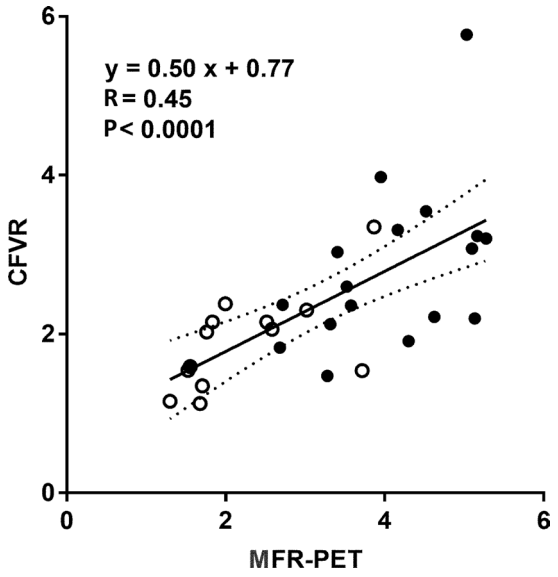

Fig. 2 Correlation and linear regression analysis between coronary flow velocity reserve (CFVR) and ^{15}O-labeled water positron emission tomography (PET) (MFR-PET). Pearson's correlation coefficients and linear regression analyses of CFVR showed positive and significant correlation with MFR-PET (R = 0.45, P < 0.0001). Black circles show healthy adults and white circles show patients with coronary artery disease.

Inter-observer calculations of CFVR showed good correlation (R^2 = 0.93, P < 0.0001).

Diagnostic value of CFVR for detection of CAD

CFVR in patients with CAD was significantly lower than that in healthy adults (1.90 ± 0.61 vs. 2.77 ± 1.03, respectively, P = 0.01) (Fig. 4a) which denoted the same tendency of the result of MFR-PET (2.23 ± 0.84 vs. 3.96 ± 1.04, respectively, P < 0.0001) (Fig. 4b).

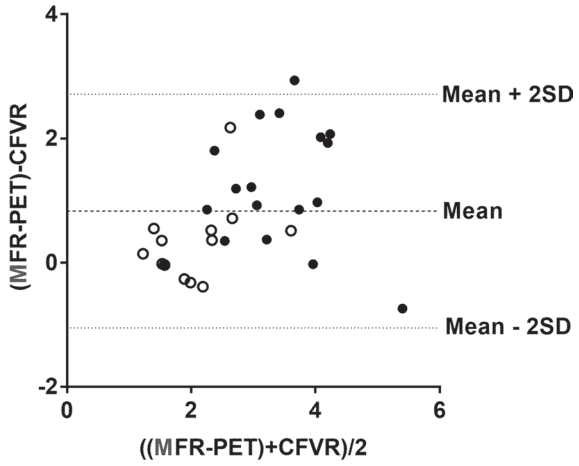

Fig. 3 Bland-Altman plot between coronary flow velocity reserve (CFVR) and ^{15}O-labeled water positron emission tomography (PET) (MFR-PET). CFVR tended to be lower than MFR-PET, and all differences of MFR-PET and CFVR were within the mean ± 2 standard deviation (SD) except for one healthy adult. Black circles show healthy adults and white circles show patients with coronary artery disease.

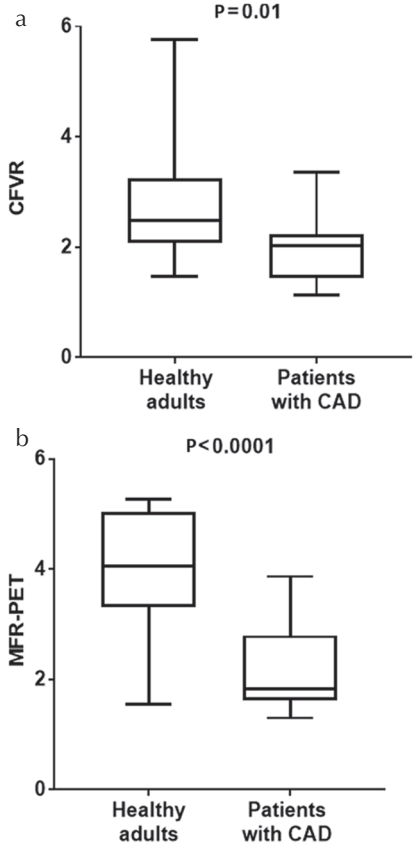

Fig. 4 Diagnostic value of coronary flow velocity reserve (CFVR) (**a**) and myocardial flow reserve (MFR) by ^{15}O-labeled water positron emission tomography (PET) (MFR-PET) (**b**) between healthy adults and patients with coronary artery disease (CAD). Patients with CAD showed significantly lower values of CFVR than those of healthy adults (1.90 ± 0.61 vs. 2.77 ± 1.03, respectively,P = 0.01) as well as the results of MFR-PET (2.23 ± 0.84 vs. 3.96 ± 1.04, respectively, $P < 0.0001$) using unpaired t-test.

In the ROC analysis of CFVR for the detection of patients with CAD, the area under the curve was 0.78 (0.95 confidence interval = 0.61-0.95, P = 0.01). The sensitivity was 0.77 and specificity was 0.72 when a cut-off of 2.15 of CFVR was used (Fig. 5).

Representative flow velocity curves during stress and at rest in a patient with CAD who had 2-VD (LAD; #6, #9 and LCx; #13) are shown in Fig. 6. The CFVR was calculated as 1.13.

Discussion

In the present study, we validated CFVR values estimated by PC MRI at 3T in comparison with MFR-PET values in both healthy adults and patients with CAD. In addition, our preliminary results showed the acceptable diagnostic value of CFVR in patients with CAD. Importantly, CFVR can be estimated without contrast material and radiation.

Although PET plays an important role in quantifying MFR using a suitable tracer kinetic model, MRI can also estimate MFR of myocardial tissue.[12] The dynamic MR perfusion method requires a gadolinium contrast material and compartment model which needs another algorithm and extra time for calculation of the MBF.[12] However, PC MRI does not need the injection of gadolinium contrast material, which can be used in patients who have contraindications for gadolinium contrast material like those with chronic kidney disease or an allergy.[18,19] MRI without contrast material has several advantages in comparison with PET for the evaluation of quantitative flow reserve. First, it is useful for patients who need serial examinations to avoid radiation exposure. Second, MRI without contrast material can assess not only CFVR but also ventricular function such as left ventricular end-diastolic or systolic volume, stroke volume, ejection fraction, and mass, regional wall contractile ability. This

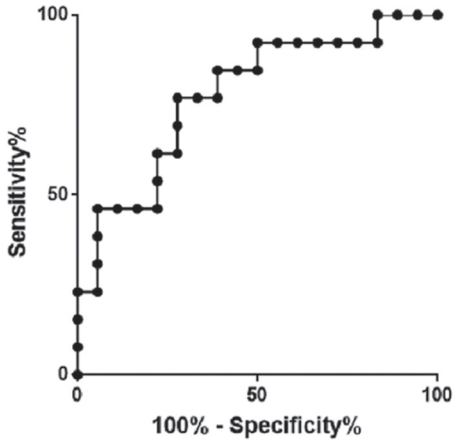

Fig. 5 Receiver operating characteristic analysis of coronary flow velocity reserve for the detection of patients with coronary artery disease (CAD). The area under the curve was 0.78 (P = 0.01). The sensitivity was 0.77 and specificity was 0.72 when a cut-off of 2.15 was used for the detection of patients with CAD.

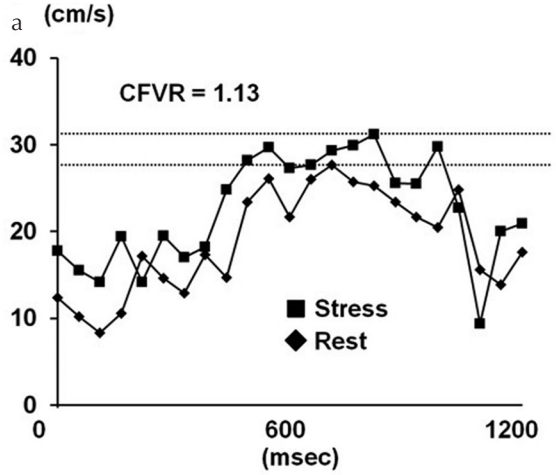

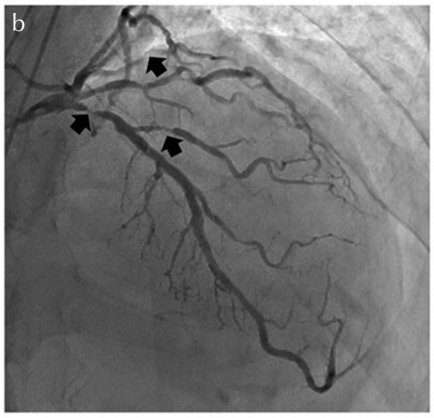

Fig. 6 A case presentation of peak-velocity curve (**a**) and invasive coronary angiography (ICA) (**b**). The patient was a 69-year-old man with an exertional chest pain. He had risk factors such as smoking, hypertension, and dyslipidemia. The coronary flow velocity reserve (CFVR) was 1.13, which was under the cut-off value (2.15) in this present study. He had 2-vessel disease (#6 99%, #9 90%, and #13 75%; arrows) on ICA.

comprehensive MRI assessment promises to improve physicians' ability to diagnose CAD.

Sakuma et al.[9] reported a CFVR estimation in the LAD using a 1.5T MR scanner compared with MFR of ^{15}O-labeled water PET for healthy adults; they showed that CFVR was correlated with the MFR of ^{15}O-labeled water PET. This was the first study to validate CFVR measured using 3T MR scanner validated in comparison with ^{15}O-labeled water PET. The usefulness of using 3T MR scanner is that the signal-to-noise ratio is more improved than 1.5T MR scanner.[20] It is enable us to distinguish easily the vessel from background noise and to keep the signal of blood flow because of the reduction of phase shift in the voxel. In addition, using 3T MR scanner has a possibility of more increases the space and time resolution than 1.5T MR scanner.

Moreover, we could shorten the imaging acquisition time using SENSE technique. The previous report wrote that they took 9-13 phases (128 ms/phase),[9] on the other hand, we took 23 phases (15.6 ms/phase). According to improve of shortening of imaging acquisition time, our accuracy of measurement can be more increased than in the past.

The diagnostic value of the measurement of CFVR in coronary artery using Doppler echocardiography or intracoronary Doppler guidewire has been shown to assess CAD.[5–8] We also showed that CFVR in patients with CAD was significantly lower than that in healthy adults in the present study although the result of patient's CFVR was preliminary. The cut-off value of CFVR 2.15 in this study is consistent with the clinical meaningful coronary flow reserve (CFR) value of 2.0 for predicting poor outcome or microcirculatory dysfunction in patients with CAD.[3,7,21–23] In this study, CFVR tended to be lower than MFR-PET. Wikström et al.[24] reported that the coronary artery lumen diameter significantly increases during stress. Because MFR on left ventricular tissue is thought to be equal to CFVR times the increase in coronary artery lumen area during stress, CFVR on the coronary artery would be lower than MFR on tissue.[24] They also reported that CFVR and MFR were positively correlated, and that CFVR could be used as an index of coronary artery function in mice.[24] We also confirmed the inter-observer consistency for calculation of CFVR and the result showed good correlation. Therefore, measurement of CFVR by MRI is acceptable and is a reliable indicator for detection of the patients with CAD.

Although CFVR measured in the distal coronary arteries has been validated in experimental studies and has been shown to have clinical utility,[25] our results evaluating CFVR on the LMT were concordant with the previous study by Han et al.[11] reported that CFVR in the proximal site of coronary stenosis was also decreased as well as that in the distal site. They also reported that increased resistance in microvasculature reflects CFVR in the LMT.[11] Presumably, the flow velocity in the LMT can be regulated by the corresponding distal coronary lumen stenosis and microvascular dysfunction.

This study has several limitations. First, the order of rest and stress examinations differed between the two modalities. In our MR protocol, imaging under the ATP-induced stress condition was performed first, followed by that at rest. In ^{15}O-labeled water PET, scans were performed in the reverse order. However, we contend that the difference in scan order between MRI and ^{15}O-labeled water PET did not significantly affect the results. Previous studies reported that there was no effects of examination order on estimated values.[12,26] Second, it is hard to take images of the RCA, which moves dynamically. However, the LMT lesion, which includes LAD and LCx lesion, supplies over 75% of the left ventricle.[10] Therefore, it is more important to assess the severity of stenosis in the left coronary arteries lesion than in the RCA lesion. In addition, we will be able to assess the CFVR on the RCA using MRI to be improved by advancement in MR techniques in the future. Third, the number of patients with CAD was small, no patients have LMT disease, and the healthy adult subjects we tested were young. However, primary objective of this study was to validate CFVR on LMT using a 3T MR scanner in relation

to MFR-PET. The values in young volunteers serve normal range of CFVR. We also showed the feasibility of this method for patients with CAD. Therefore, future study with more emphasis on patients with CAD is warranted. Finally, we used the results of ICA, but not magnetic resonance coronary angiography (MRCA) in this study. We need to evaluate not only CFVR and also the coronary stenosis using MRCA as a prospective study in the future.

Conclusion

We have validated CFVR assessed by PC MRI at 3T in comparison with MFR-PET with ^{15}O-labeled water PET in both healthy adults and patients with CAD. CFVR is feasible to detect the patients with CAD without radiation or contrast material.

Acknowledgment

The authors thank Yuuki Tomiyama, PhD, and Chietsugu Katoh, MD, PhD, for support. In addition, this research is partly supported by JSPS KAKENHI (contract grant number: 40443957), Japan Radiological Society Bayer Grant (to O.M.).

Conflicts of Interest

There is no conflict of interest related to this work.

References

1. White CW, Wright CB, Doty DB, et al. Does visual interpretation of the coronary arteriogram predict the physiologic importance of a coronary stenosis? N Engl J Med 1984; 310:819–824.
2. Naya M, Di Carli MF. Myocardial perfusion PET/CT to evaluate known and suspected coronary artery disease. Q J Nucl Med Mol Imaging 2010; 54:145–156.
3. Kikuchi Y, Oyama-Manabe N, Naya M, et al. Quantification of myocardial blood flow using dynamic 320-row multi-detector CT as compared with ^{15}O-H_2O PET. Eur Radiol 2014; 24:1547–1556.
4. Naya M, Murthy VL, Taqueti VR, et al. Preserved coronary flow reserve effectively excludes high-risk coronary artery disease on angiography. J Nucl Med 2014; 55:248–255.
5. Wada T, Hirata K, Shiono Y, et al. Coronary flow velocity reserve in three major coronary arteries by transthoracic echocardiography for the functional assessment of coronary artery disease: a comparison with fractional flow reserve. Eur Heart J Cardiovasc Imaging 2014; 15: 399–408.
6. Ruscazio M, Montisci R, Colonna P, et al. Detection of coronary restenosis after coronary angioplasty by contrast-enhanced transthoracic echocardiographic Doppler assessment of coronary flow velocity reserve. J Am Coll Cardiol 2002; 40:896–903.
7. Daimon M, Watanabe H, Yamagishi H, et al. Physiologic assessment of coronary artery stenosis by coronary flow reserve measurements with transthoracic Doppler echocardiography: comparison with exercise thallium-201 single piston emission computed tomography. J Am Coll Cardiol 2001; 37:1310–1315.
8. Claessen BE, Bax M, Delewi R, Meuwissen M, Henriques JP, Piek JJ. The Doppler flow wire in acute myocardial infarction. Heart 2010; 96:631–635.
9. Sakuma H, Koskenvuo JW, Niemi P, et al. Assessment of coronary flow reserve using fast velocity-encoded cine MR imaging: validation study using positron emission tomography. AJR Am J Roentgenol 2000; 175:1029–1033.
10. Cheng HY, Wang KT, Lin WH, Tsai JP, Chen YT. Percutaneous coronary intervention for left main coronary artery disease - a single hospital experience without on-site cardiac surgery. Acta Cardiol Sin 2015; 31:267–279.
11. Han B, Wei M. Proximal coronary hemodynamic changes evaluated by intracardiac echocardiography during myocardial ischemia and reperfusion in a canine model. Echocardiography 2008; 25:312–320.
12. Tomiyama Y, Manabe O, Oyama-Manabe N, et al. Quantification of myocardial blood flow with dynamic perfusion 3Tesla MRI: validation with ^{15}O-water PET. J Magn Reson Imaging 2015; 42:754–762.
13. Mueller A, Kouwenhoven M, Naehle CP, et al. Dual-source radiofrequency transmission with patient-adaptive local radiofrequency shimming for 3.0-T cardiac MR imaging: initial experience. Radiology 2012; 263:77–85.
14. Sakuma H, Blake LM, Amidon TM, et al. Coronary flow reserve: noninvasive measurement in humans with breath-hold velocity-encoded cine MR imaging. Radiology 1996; 198:745–750.
15. Katoh C, Morita K, Shiga T, Kubo N, Nakada K, Tamaki N. Improvement of algorithm for quantification of regional myocardial blood flow using ^{15}O-water with PET. J Nucl Med 2004; 45:1908–1916.
16. Jiang J, Kokeny P, Ying W, Magnano C, Zivadinov R, Mark Haacke E. Quantifying errors in flow measurement using phase contrast magnetic resonance imaging: comparison of several boundary detection methods. Magn Reson Imaging 2015; 33:185–193.
17. Shibata M, Sakuma H, Isaka N, Takeda K, Higgins CB, Nakano T. Assessment of coronary flow reserve with fast cine phase contrast magnetic resonance imaging: comparison with measurement by Doppler guide wire. J Magn Reson Imaging 1999; 10:563–568.
18. Thomsen HS. Nephrogenic systemic fibrosis: a serious adverse reaction to gadolinium - 1997-2006-2016. Part 2. Acta Radiol 2016; 57:643–648.
19. Thomsen HS. Nephrogenic systemic fibrosis: a serious adverse reaction to gadolinium - 1997-2006-2016. Part 1. Acta Radiol 2016; 57:515-520.
20. Miyazaki M, Akahane M. Non-contrast enhanced MR angiography: established techniques. J Magn Reson Imaging 2012; 35:1–19.
21. Miller DD, Donohue TJ, Younis LT, et al. Correlation of pharmacological 99mTc-sestamibi myocardial perfusion

imaging with poststenotic coronary flow reserve in patients with angiographically intermediate coronary artery stenoses. Circulation 1994; 89:2150–2160.
22. Matsumura Y, Hozumi T, Watanabe H, et al. Cut-off value of coronary flow velocity reserve by transthoracic Doppler echocardiography for diagnosis of significant left anterior descending artery stenosis in patients with coronary risk factors. Am J Cardiol 2003; 92:1389–1393.
23. Kawata T, Daimon M, Hasegawa R, et al. Prognostic value of coronary flow reserve assessed by transthoracic Doppler echocardiography on long-term outcome in asymptomatic patients with type 2 diabetes without overt coronary artery disease. Cardiovasc Diabetol 2013; 12:121.
24. Wikström J, Grönros J, Gan LM. Adenosine induces dilation of epicardial coronary arteries in mice: relationship between coronary flow velocity reserve and coronary flow reserve in vivo using transthoracic echocardiography. Ultrasound Med Biol 2008; 34: 1053–1062.
25. Segal J, Kern MJ, Scott NA, et al. Alterations of phasic coronary artery flow velocity in humans during percutaneous coronary angioplasty. J Am Coll Cardiol 1992; 20: 276–286.
26. Furuyama H, Odagawa Y, Katoh C, et al. Altered myocardial flow reserve and endothelial function late after Kawasaki disease. J Pediatr 2003; 142:149–154.